AAPG Annual Convention
Salt Lake City, Utah
May 11-14, 2003

Genesis of mass wasting seismic facies deduced by CAT-scan analysis.

DUCHESNE, MATHIEU JACQUES and LONG, BERNARD FRANÇOIS, National Research Institute on Water, Earth and Environment, Canada

Introduction

Some authors have demonstrated that the coupling of CAT-scan with seismic data can be a useful tool in sedimentology (Schillinger, 2000; Abegg and Anderson, 1997). This coupling has been used by Abbeg and Anderson (1997) to study the relationship between CH_4 bubble distribution in fine-grained sediments and the observation of turbid acoustic units. Long and Schillinger (2001) and Schillinger (2000) have used the analogy between CAT-scan data and seismic facies to study the architecture of an intertidal sand body. However, concerning the analysis of submarine mass wasting deposits no correlation has ever been made between CAT-scan and seismic signatures. Some authors have demonstrated that CAT-scan is a powerful tool to reveal mm-scale stratigraphy (Boespflug et al., 1995; Occhietti et al., 1995). The very-high resolution of the CAT-scan can thus help to better understand the seismic signature of the sediments.

During 2001 and 2002 four surveys were conducted in the Upper Saguenay Fjord basin, Canada, and have permitted to obtain numerous piston cores and more than 1000 km of very-high-resolution seismic profiles. Seismic line positioning accuracy was 1 m (DGPS) and core positioning accuracy was between 2 and 12 m (Track Point II). The Upper Saguenay Fjord basin, has been struck in the last ~400 yrs by catastrophic sedimentation episodes (Crémer et al., 2002; Locat et al., 2001; Syvitski and Schaffer, 1996; Praeg and Syvitski, 1991). Some authors have hypothesized that most of the seafloor failures and mass wasting deposits located in this area, are the result of the 1663 $M_s \sim 7$ Charlevoix earthquake (Syvitski and Schafer, 1996). According, to Syvitski and Schafer (1996) this event has generated an amalgamation of 100 m thick mass wasting deposits on the basin floor. Therefore, this area represents a unique site to study the genesis of modern mass wasting deposits.

The main objective of this project is to determine the genesis and the sedimentary architecture of some mass wasting deposits seismic facies within the study area, by CAT-scan analysis. However in this paper, only the relation between some mass wasting deposits seismic facies and CAT-scan facies is discussed.

Correlations between seismic facies and CAT-scan imagery : an example.

Methodology

Several 2-D seismic profiles were collected with an IKB-Seistec (3.5 kHz, 175 J) over the study area with a 20 m spacing. Coring sites were surveyed with two perpendicular 2-D seismic profiles. Sampling rate during seismic data acquisition was 20 μs. This high sampling rate has permitted to build each seismic wavelet from 13 amplitude values. Wavelength of each wavelet is ~0.26 ms or ~0.2 m which corresponds to the resolution of the survey. Seismic signal attenuation by the water column at the coring site is 0.04 dB. Geometrical spreading attenuation of the seismic signal at 150 m of water depth is 49.5 dB. Seismic lines were processed with Kingdom Suite seismic software package.

All cores samples were analyzed with a fourth generation Siemens Somatom Volume Access medical CAT-scan at the Multidisciplinary CAT-scan Laboratory of Quebec, Canada. It has provided 1 mm resolution axial topograms of the cores. The topograms represent X-rays linear attenuation coefficients distribution maps of the various core sections over their longitudinal axis. The topogram imagery shows a 2-D mean linear attenuation coefficient pixel matrix (each pixel=1$\times$1 mm) obtained by integrating coefficient values over the total thickness of the core (10 cm) in the perpendicular axis of the core. Core logging was made based on image textures and density contrasts expressed by gray level variations. Each core topogram had a width of 100 pixels. Hounsfield unit (HU) spectrums were obtained by computing an HU mean value on a 20 pixels width centered on pixel 50. The 20 pixels width was chosen to calculate the mean instead of the total width of the core (100 pixels), to avoid the integration of a smaller number of coefficients because the core is thinner near its border. Because of the rapid fluctuations of the HU values and the noisy character of the spectrums, all spectrums were smoothed with a Daubechies wavelet transform. Beam-hardening artifacts, caused by important density contrasts (air vs sediments) at both ends of each core sections, were easily removed prior to the smoothing. The beam-hardening effect has been observed in media with important density contrasts; e.g. at the interface of mud and highly compacted sand layers (Duliu, 1999). Based on the HU spectrum observations there is no major density contrast that can be related to the beam-hardening effect. For the selected core, HU values range between 1021.39 and 1229.4 HU.

Prior to the correlations, work flow included: 1) extraction of the seismic traces corresponding to each core location with the Kingdom Suite seismic software package, 2) depth to time conversion for all cores to assess a correct correspondence between the seismic trace and HU spectrum, 3) seismic facies description and interpretation and 4) CAT-scan facies description and interpretation. Then, for each core, qualitative correlations between the seismic trace and the HU spectrum, between the seismic trace, the CAT-scan image, and the HU profile were completed. Because the core positioning accuracy ranges from 2 to12 m and because shot point spacing is ~ 1 m, an average seismic trace was computed based on the summation of 12 seismic traces (6 traces on each side of the coring site) from the acoustic impedance values corresponding to the core length.

Seismic and CAT-scan data descriptions

Core MB01-03 is 5.45 m (7.3 ms) long and has been sampled in mass wasting deposits. This core was chosen because of its important vertical facies variations. Table 1 shows core MB01-03 CAT-scan facies characteristics. Figure 1 I) shows core location on the corresponding seismic profile. On this profile, six different seismic horizons of higher amplitudes have been pin pointed as seismic markers respectively at 126 (marker a), 123.9 (marker b), 122.5 (marker c), 121.2 (marker d), 120.1 (marker e), and 119.4 ms (marker f) (figure 1 I)). The core penetrates three different seismic facies. The first facies corresponds to low amplitude chaotic reflections and transects the core on length of 3.1 m (4 ms). This facies is delimited at the base by a series of hummocky reflectors and at the top by a medium amplitude chaotic reflector. The second facies is represented by a series of wavy to chaotic reflections which have amplitudes ranging from medium to high. This facies is 1.60 m (2.1 ms) thick. The last facies lies sharply on the previous one and is imaged by a series of high amplitude undulating reflectors. It represents the top 0.9 m (1.20 ms) of the core.

Table 1: CAT-scan facies characteristics.

Facies	Thickness (cm)	Contacts	Remarks
Matrix supported (Ms)	93.8	Top: sharp	Low density fine matrix
Low density laminated/Matrix supported (LDl/MS)	122.8	Bottom: gradual Top: sharp	3mm thick laminae, ribbon-like texture, coarse particles oriented on their long axis
Low density laminated/ Low density massive (LDl/LDm)	140	Bottom: gradual Top: gradual	More laminated near the base
High density laminated/High density massive (HDl/HDm)	8.8	Bottom: gradual Top: sharp	4mm thick laminae
High density laminated (HDl)	13.3	Bottom: sharp Top: sharp	Undulated bottom contact
Matrix supported (Ms)	17.6	Bottom: sharp Top: sharp	High density coarse matrix
High density laminated (HDl)	11	Bottom: sharp Top: sharp	Undulated bottom contact
Low density laminated/Low density massive (LDl/LDm)	15	Bottom: sharp Top: sharp	2mm thick laminae, bioturbated, normal grading
Low density laminated/ high density laminated (LDl/HDl)	11	Bottom: sharp Top: sharp	3mm thick laminae, bioturbated, reverse grading, high rhythmicity
Low density laminated/ Low density massive (LDl/LDm)	13	Bottom: sharp Top: gradual	Bioturbated, reverse grading
Matrix supported (Ms)	84	Bottom: gradual Top: sharp	Low density fine matrix
High density laminated (HDl)	2	Bottom: sharp Top: sharp	Sheet-like appearance
Matrix supported (Ms)	5	Bottom: sharp Top: sharp	Low density fine matrix
High density laminated (HDl)	8	Bottom: sharp	Deformations caused by the corer

Correlations
Figure 1 II) shows qualitative correlations between the CAT-scan imagery and spectrum and the corresponding average acoustic impedance trace. Correlations between the acoustic markers and the CAT-scan imagery does not show clear links. Only one of the six acoustic markers has been identified on the CAT-scan imagery and CAT-scan HU spectrum (figure 1 II)). However, correlations between CAT-scan imagery and the acoustic impedance trace are more revealing; 10 peaks or troughs of the acoustic impedance trace roughly correspond to abrupt changes on the HU spectrums and to CAT-scan facies variations (figure 1 II)).

The same type of correlations were made at a greater scale of the core between 200 and 86 cm where abrupt facies variations were documented (figure 1 III)). Seven different facies were observed on this section (table 1). Correlations show that some CAT-scan facies and HU spectrum oscillations match with peaks and troughs of the acoustic impedance trace. The figure 1 III) images sub-facies and facies variations that are ignored by the acoustic impedance trace. Two successive wavelets (wavelets A and B on figure 1 III)) between 162.1 and 117.22 cm show the same maximum amplitudes; i.e. 241.9. However, their correlations with the HU spectrum and the CAT-scan imagery reveal different facies natures. The peak of wavelet A is represented by a low density laminated/low density massive facies and the peak of wavelet B by a matrix-supported facies.

The first seismic facies (see figure 1 I)) corresponds on the CAT-scan imagery to three distinct CAT-scan facies. The chaotic reflections are typical of debris flow sedimentation (Hart et al., 1992; Berryhill et al., 1987). The matrix supported facies observed on the CAT-scan imagery are also characteristic of debris flow sedimentation (Ghidaubo, 1992). The ribbon-like textures may represent internal shearing deformation within the failing mass (Major, 1997). The long axis orientation of the coarse grain particles have been previously interpreted by Major (1998) as an evidence of shearing caused by the stacking of the different flow pulsations in a debris flow. The second seismic facies related to nine CAT-scan facies, is also typical of a debris flow deposition. Nevertheless, the CAT-scan data suggest other sedimentary processes to explain the sedimentation of these facies. High density laminated facies can be attributed to upper-flow regime transport and high density massive facies might be linked to grain flow sedimentation (Shanmugam, 1997; Allen, 1984). The low density laminated and massive facies can represent the settling out of suspended sediment plumes (Galloway, 1998). These plumes are generated when the energy released by a collapsing mass and its subsequent transformation into a debris flow, tends to push the fine and less consolidated sediments outward and upward in the water column. Then, these sediments are deposited from suspension. The third seismic facies includes four different CAT-scan facies. This seismic facies is more coherent with the CAT-scan facies and it translates the stratifications of the upper sediment column even if it includes the top section of the matrix supported facies. The sharp facies contacts which are sometimes undulating are scour surfaces. These scour surfaces represent the passage of various flows which, based on the CAT-scan imagery, are also of different natures.

Discussion
Acoustic impedance is directly related to the sediments density. Seismic traces show density contrasts expressed by amplitude intensity variations. The density is a function of several parameters such as gas content, water content, mineralogy and porosity. All these parameters contribute to the seismic trace attenuation. On the other side, CAT-scan signal is also related to the sediments density. As for the acoustic impedance, the same parameters can play an important role on X-rays linear attenuation. In addition, photoelectric and Compton effects cannot be overlooked in the analysis of CAT-scan response (Duliu, 1999). Concerning the photoelectric effect, the chemical composition of the absorbing matter affects the X-ray linear attenuation and is influenced by high atomic number elements. It is particularly the case for carbonate sediments where calcium (Ca) enhances X-ray linear absorption (Boespflug et al., 1995). The Compton effect is characterized by the deviation of a part of the X-ray beam and by the frequency variation of certain rays of the deflected beam. It has been postulated, that the Compton effect can be constraining in high porosity and high gas content media. Neither of the two effects have modified both the CAT-scan imagery and the HU spectrum on core MB01-03 because 1) the source rocks of the area are mainly composed of granite and anorthosite and 2) based on the HU spectrum analysis porosity and gas content are not important (air=-1000 HU and water=0 HU).

The presence of strong tidal currents on the surveyed site has contributed to a lack of accuracy in the core positioning. This lack of accuracy can explain the absence of clear links between the seismic markers and the CAT-scan imagery. As a matter of fact, a more accurate core positioning could avoid the necessity of computing an average seismic trace to match the core location. Knowing the study area is characterized by rapid lateral facies variations (see Duchesne et al., 2003) positioning accuracy is even more important. Thus, the average seismic trace can represent the summation of the acoustic response of these facies variations instead of the core's different facies acoustic response.

The different resolution of both tools used can also help to clarify the small number of correlations between the seismic markers and the CAT-scan imagery. Even with the high sampling frequency of the survey, amplitude values were recorded every ~15 mm which is ~15 times lower than the HU spectrum and the CAT-scan imagery resolution. It can explain why very-fine stratigraphy highlighted by the CAT-scan analysis could not been resolved by the seismic profiling. These amplitude values were taken at a constant sampling rate which does not encompass amplitude variations over the 15 mm spacing between the sampled values. Thus, the seismic trace cannot image facies variations by means of amplitudes below the sampling rate resolution.

In the present case, the seismic attenuation caused by the water column is not an aggravating factor but geometrical spreading of the seismic impulsion is believe to be more problematic considering the source energy and water column thickness. Geometrical spreading is the second cause of signal attenuation after sound absorption by the sediments (Urick, 1983). Geometrical spreading is directly related to the insonified area which is ~20 m for the surveyed sector. This effect averages out the data resulting in loss of resolution and in generation of artifacts (e.g. seismic facies layering modification) (Mosher and Simpkin, 1999). CAT-scan measurements have a rectangular shape. Seismic measurements taken from any acoustic device are a function of the effective beamwidth of the source which means that a seismic trace includes echoes from a conical volume of sediment (Urick, 1983). Therefore, the source beamwidth geometry may have induced artifacts that can mislead correlation interpretations.

Finally, piston coring does not properly recover the first m or so of sediments. Buckley et al. (1994) have mentioned a series of incidents related to piston coring activity such as foreshortening and stretching of sedimentary units mainly caused by pressure fluctuations inside the core liner. So, when it comes to correlate seismic with CAT-scan data it can generate a correlation offset because the core thickness does not correspond to the "real" depth in the sedimentary column.

Nevertheless, this study has shown that similar mass wasting seismic facies and same amplitude wavelet peaks can correspond to different CAT-scan facies. Consequently, different CAT-scan facies can give the same acoustic response. CAT-scan observations have permitted to explain fine-scale changes in seismic facies. The resolving of mm scale beds has helped to better understand the seismic expression of mass wasting deposits. This paper presented the first step of more extensive study on correlations between seismic and CAT-scan data. Subsequent steps will focus on the correlations of CAT-scan observations of sedimentary facies packages with seismic facies. Moreover, a wider variety of seismic and CAT-scan facies will be analyzed, in order to use fine-scale stratigraphy derived by CAT-scan to determine very-fine seismic analogs.

Acknowledgements

This research was funded by the National Scientific and Engineering Research Council of Canada. The authors would also like to express their gratitude to Peter G. Simpkin (IKB Technology) for is technical support during and after the surveys, to Sharon Pearsons for reviewing this manuscript and to Seismic Micro-Technology for providing the Kingdom Suite seismic software package.

References

Abegg, F. and Anderson, A. L. 1997. The acoustic turbid layer in muddy sediments of Eckenfoerde Bay, western Baltic; methane concentration, saturation and bubble characteristics. Marine Geology, 137: 137-147.

Allen, J. R.L. 1984. Laminations developed from upper-stage plane beds: A model based on the larger coherent structures of the turbulent boundary layer. Sedimentary Geology, 39: 227-242.
Berryhill, H. L. jr, Suter, J. R. and Hardin, N. S. 1987. Late Quaternary Facies and Structure, Northern Gulf of Mexico : Interpretation from Seismic Data. AAPG Studies in Geology #23, Tulsa, 289 pages.
Boespflug, X., Long, B. F. N. and Occhietti, S. 1995. CAT-scan in marine stratigraphy: a quantitative approach. Marine Geology, 122: 281-301.
Buckley, D. E., MacKinnon, W. G., Cransto, R. E. and Christian, H. A. 1994. Problems with piston core sampling: Mechanical and geochemical diagnosis. Marine Geology, 117: 95-106.
Crémer, J.-F., Long, B., Desrosiers, G., de Montety, L. and Locat, J. 2002. Application de la scanographie à l'étude de la densité des sédiments déposés dans la rivière Saguenay (Québec, Canada) après la crue de juillet 1996. Canadian Geotechnical Journal, 39: 440-450.
Duchesne, M. J., Long, B. F., Locat, P., Locat J. and Massé, M. *in press*. The Pointe-du-Fort mass movements deposits, Upper Saguenay Fjord, Canada: a multiphase build-up. *In* Submarine Mass Movements and their Consequences. *Edited by* J. Locat, Kluwer Academic Publishers, Dordrecht.
Duliu, O. G. 1999. Computer axial tomography in geosciences : an overview. Earth-Science Reviews, 48: 265-281.
Galloway, W.E. 1998. Siliclastic slope and base-of-slope depositional systems : component facies, stratigraphic architecture, and classification. AAPG Bulletin, 82 : 569-595.
Ghidaubo, G. 1992. Subaqueous sediment gravity flow deposits: practical criteria for their field interpretation and classification. Sedimentology, 39: 423-454.
Hart, B. S., Prior, D. B., Barrie, J. V., Currie, R. G. and Luternauer, J. L. 1992. A river mouth submarine channel and failure complex, Fraser Delta, Canada. Sedimentary Geology, 81: 73-87.
Locat, P., Locat, J., Leroueil, S., Urgeles, R., Hart, B. and Long, B 2001. Caractérisation préliminaire du glissement sous-marin de la Pointe-du-Fort, Fjord du Saguenay, Québec, Canada. *In* Proceedings of the 2nd Join Conference of the International Association of Hydrogeologists and the Canadian Geotechnical Society, pp. 752-759.
Long, B. F. and Schillinger, S. 2001. Détermination des facies sédimentaires de flèches intertidales par tomographie axiale. *In* Proceedings of the 2001 Canadian Coastal Conference May 16-19 2001. *Edited by* B. F. Long, pp. 447-463.
Major, J. J. 1997. Depositional Processes in large scale debris-flow experiments. Journal of geology, 105: 345-366.
Major, J. J. 1998. Pebble orientation on large, experimental debris flow deposits. Sedimentary Geology, 117: 151-164.
Mosher, D. C. and Simpkin, P. G. 1999. Status and trends of marine high-resolution seismic reflection profiling: data acquisition. Geoscience Canada, 26: 174-188.
Occhietti, S., Long, B., Clet, M., Boespflug, X. and Sabeur, N. 1995. Séquence de la transition Illinoen-Sangamonien: forage IAC-91 de l'Ile aux Coudres, estuaire moyen du Saint-Laurent, Québec. Canadian Journal of Earth Sciences, 32: 1950-1964.
Praeg, D. B. and Syvitski, J. P. M. 1991. Marine geology of Saguenay Fjord. Geological Survey of Canada, Bedford Institute of Oceanography, Dartmouth, Open File #2395, 14 maps.
Schillinger, S. 2000. Genèse et architecture d'une fleche sableuse: le banc du Bûcheron, Ile de Ré. Ph.D. Thesis. Université du Québec à Rimouski, 226 pages.
Shanmugam, G. 1997. The Bouma sequence and the turbidite mind set. Earth-Science Reviews, 42: 201-229.
Syvitski, J. P. M. and Schafer, C. T. 1996. Evidence of an earthquake-triggered basin collapse in Saguenay, Fjord, Canada. Sedimentary Geology, 104 : 127-153.
Urick, R. J. 1983. Principles of Underwater Sound. McGraw-Hill Book Company, New York, 423 pages.

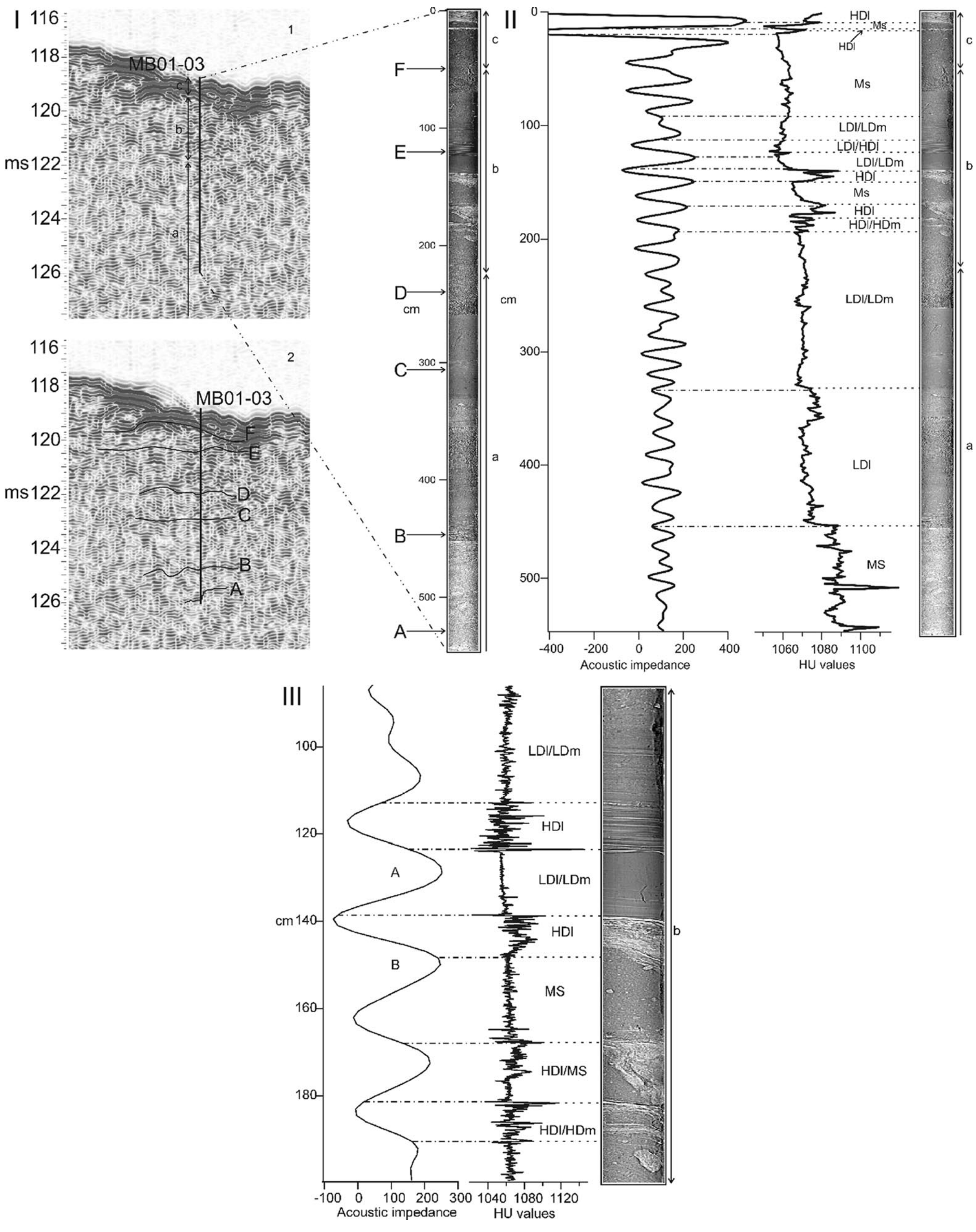

Figure 1. Correlations between seismic and CAT-scan facies. I) (1) Correlations between seismic facies and CAT-scan facies (lowercase letters) and (2) position of the seismic markers on the core (capital letters). **II** Correlations between the average seismic trace, the HU spectrum and CAT-scan facies. Lowercase letters indicate the corresponding seismic facies. See table 1 for symbols signification. **III**-Small scale correlations between the average seismic trace, the HU spectrum and CAT-scan facies. See table 1 for symbol signification. b indicates the corresponding seismic facies. Capital letters represent discussed wavelets. Note that the HU spectrum is has not been smoothed with a wavelet transform.